

Organic matter pools in sediments of the tidal Elbe river

Zander, F.; Groengroeft, A.; Eschenbach, A.; Heimovaara, T. J.; Gebert, J.

DOI

[10.1016/j.limno.2022.125997](https://doi.org/10.1016/j.limno.2022.125997)

Publication date

2022

Document Version

Final published version

Published in

Limnologica

Citation (APA)

Zander, F., Groengroeft, A., Eschenbach, A., Heimovaara, T. J., & Gebert, J. (2022). Organic matter pools in sediments of the tidal Elbe river. *Limnologica*, 96, Article 125997. <https://doi.org/10.1016/j.limno.2022.125997>

Important note

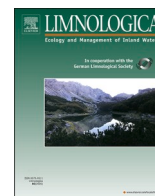
To cite this publication, please use the final published version (if applicable). Please check the document version above.

Copyright

Other than for strictly personal use, it is not permitted to download, forward or distribute the text or part of it, without the consent of the author(s) and/or copyright holder(s), unless the work is under an open content license such as Creative Commons.

Takedown policy

Please contact us and provide details if you believe this document breaches copyrights. We will remove access to the work immediately and investigate your claim.



Organic matter pools in sediments of the tidal Elbe river

F. Zander^{a,*}, A. Groengroeft^b, A. Eschenbach^b, T.J. Heimovaara^a, J. Gebert^a

^a Delft University of Technology, Dept. Geoscience and Engineering, Stevinweg 1, 2628 CN Delft, the Netherlands

^b University of Hamburg, Dept. Department of Earth Sciences, Allende-Platz 2, 20146 Hamburg, Germany

ARTICLE INFO

Keywords:

Organic matter decay rates
Organic matter lability
Recalcitrance
Spatial variability
River sediments

ABSTRACT

Anaerobic sediment organic matter decay generates methane, delays sediment consolidation, reduces sediment density, viscosity and shear strength, all impacting the sediment rheological parameters and the navigable depth. This study quantifies the share of anaerobically and aerobically degradable sediment organic matter (SOM) in a depth profile and along a transect through the tidal river Elbe in the section of the Port of Hamburg. From exponential organic matter decay functions, organic matter decay rates ($\text{mg C g}_{\text{TOC}}^{-1} \text{d}^{-1}$) were derived and clustered with a k-Means Cluster Analysis. The reactivity of different (kinetic) organic matter pools along the river transect were characterized based on their biodegradation rates. A fast, medium, slowly and non-degradable pool (pools 1–4) were identified based on the measured organic matter lability. SOM lability decreased from upstream to downstream, evidenced by the decreasing amount of the easily degradable pool 1 material from upstream to downstream. The size of the slowly degradable pool 3, assumed to be associated with SOM bound to the mineral particles, did not show any spatial gradient and is therefore suggested to represent a baseline share of hardly accessible SOM in the investigation area (about 12%–16% of TOC). Total degradability thus appears to be governed by the amount of SOM present in addition to this basis (pool 3), which in turn follows a source gradient and an age gradient from upstream to downstream. The recalcitrant pool 4 was the largest at any part of the harbour, for any depth, and for both, anaerobic and aerobic conditions (about 75%–85% of TOC). This indicates that the sediment in the investigation area, including the uppermost fluidic and freshly settled layers, mostly comprises stabilised organic matter and contributes largely to storage of organic carbon. Differently sized anaerobic SOM pools with depth were observed as well as seasonal changes of the easily degradable SOM pool 1. The degradability was larger in upper sediment layers, it was also larger under aerobic conditions (by about 10% of TOC) but the differences between aerobic and anaerobic decay decreased from upstream to downstream.

1. Introduction

Organic matter interacts with the sediment mineral phase through Van der Waal's or Coulombic forces. By bridging mineral particles and thereby promoting floc formation (Deng et al., 2019), organic matter can enhance settlement of suspended particulate matter (SPM). Shakeel et al. (2019) showed that organic matter increased the yield points (shear stresses) of freshwater Elbe sediments at a given density while Wurpts and Torn (2005) contend that microbially formed extrapolymeric substances (EPS) decrease yield point and viscosity of saline fluid mud layers in Emden seaport. EPS have been shown to profoundly influence bedform dynamics, increasing the time for development of

bedforms for small quantities of EPS (Malarkey et al., 2015; Parsons et al., 2016). Sills and Gonzalez (2001) and Jommi et al. (2019) have demonstrated strong reduction in shear stresses by gas originating from organic matter decay. The (anaerobic) decay of organic matter leads to the generation of methane gas, delays sediment consolidation, reduces sediment density, viscosity and shear strength (Shakeel et al., 2022; Zander et al., 2022), impacting flow properties and therefore the navigable depth. Given the effects organic matter can exert on the physical behaviour of fine-grained sediment (mud), it is of interest to assess its lability, or, inversely, its stability or recalcitrance towards microbial degradation.

Microbial degradation of sediment organic matter (SOM) is part of

* Correspondence to: Faculty of Civil Engineering and Geosciences, Department of Geoscience & Engineering, Delft University of Technology, Stevinweg 1, 2628 CN Delft, the Netherlands.

E-mail addresses: f.zander@tudelft.nl (F. Zander), Alexander.Groengroeft@uni-hamburg.de (A. Groengroeft), Annette.Eschenbach@uni-hamburg.de (A. Eschenbach), T.J.Heimovaara@tudelft.nl (T.J. Heimovaara), j.gebert@tudelft.nl (J. Gebert).

<https://doi.org/10.1016/j.limno.2022.125997>

Received 16 November 2021; Received in revised form 16 May 2022; Accepted 8 June 2022

Available online 30 June 2022

0075-9511/© 2022 The Authors. Published by Elsevier GmbH. This is an open access article under the CC BY license (<http://creativecommons.org/licenses/by/4.0/>).

the natural aquatic carbon cycle. SOM degradation and, complementary, burial of non-degraded SOM, depends on the amount of organic matter, its intrinsic lability, environmental conditions driving microbial activity and the availability of terminal electron acceptors (for a review see Arndt et al., 2013). Phyto- and zooplankton biomass is an important source of labile organic matter in aquatic systems (van Duyl et al., 1999; Tillmann et al., 2000; Wolfstein et al., 2000), providing autochthonous, easily degradable organic matter (Grasset et al., 2018) to the system. Boyd et al. (2013) showed this fraction to be readily degraded under both, anoxic and oxic, conditions. Similarly, McKew et al. (2013) found that in estuarine sediments, the anaerobic community could rapidly utilise labile biofilm DOC and EPS at the same rates as the aerobic community. For the investigated transect through the Port of Hamburg, the source area for labile organic matter is the non-tidal shallow, eutrophic upstream river section with enhanced net primary production, whereas the significantly deeper waters of the Hamburg Port area are characterized by light-deficiency induced decay of algal biomass and zooplankton grazing (Schoel et al., 2014). For a section of about 200 km upstream of the Port of Hamburg, Kamjunke et al. (2021) coupled phytoplankton biomass to solar irradiation and low river discharge, inducing less mixing within the water column. They showed that it was hampered by nutrient dynamics only when biomass concentrations were high. In downstream sections of the Elbe River, the share of particulate organic material decreased, indicating decomposition in the upper estuary and dilution with inorganic SPM from the lower estuary (Brockmann, 1994). Easily degradable organic matter of marine phytoplankton origin hardly reaches the investigated section as it is already degraded during its upstream-directed passage through the zone of maximum turbidity (Wolfstein and Kies, 1999).

In addition to autochthonous, labile organic matter the investigation area also receives allochthonous organic matter bound to mineral particles originating from the North Sea with (Kappenberg and Fanger, 2007; Zander et al., 2020), due to its location in the tidal section of the Elbe river. This share is stabilized in organo-mineral complexes in which organic matter is less accessible to microbial decay (Baldock and Skjemstad, 2000; Six and Paustian, 2014; Gao et al., 2019). Although significantly lower carbon release rates can therefore be expected from the microbial decay of this organic matter fraction, its high mass as part of the mineral sediment inventory makes it an important pool in the overall sediment carbon budget. For many estuaries, fundamental data gaps hamper the understanding of the connectivity of terrestrial, aquatic and marine carbon budgets (Ward et al., 2015).

When organic matter is degraded under aerobic conditions in the water column or close to the sediment-water interface and the aerobic microbial activity exceeds the rate of oxygen supply, oxygen depleted zones can form in the water column (Rabalais et al., 2010). Die-off of upstream riverine phytoplankton in downstream areas led to oxygen depleted zones in the Elbe river (Geerts et al., 2017). Grasset et al. (2021) found that the methane production, resulting from anaerobic sediment organic matter decay, increased linearly with the quantity of phytoplankton-derived and terrestrially-derived organic matter. The methane production correlated strongly and positively with the amount of organic matter supply and negatively with the C/N ratio. Technical problems arising from methane-enriched sediment include impeded nautical depth finding due to reflection of sonic waves and risks of explosion in the suction head and on board of trailing suction hopper dredgers. From various perspectives it is therefore of interest to understand the drivers and mechanisms of organic matter decay in river sediments as well as the size of degradable organic matter pools.

Earlier investigations, using sediment data from the Port of Hamburg from 2018, revealed spatial gradients of SOM decay in the tidal Elbe river around the Port of Hamburg, with a gradient of decreasing SOM decay from upstream to downstream and with depth/age (Zander et al., 2020). SOM decay kinetics in all layers mostly showed an asymptotic behaviour with rates decreasing exponentially over time. For many samples, the data were best described by applying multiphase (mostly

two phase) exponential decay models. This suggested that also in these freshwater sediments discrete organic matter pools with specific decay rate constants exist, proposed earlier by Boudreau and Ruddick (1991), which decrease over time, as shown by Westrich and Berner and references therein (1984) for freshwater phytoplankton, and by Jørgensen (1979, 1982) and Middelburg (1989) for marine sediments. As a result, more recalcitrant organic matter components progressively accumulate (Burdige, 2007; Middelburg and Meysman, 2007).

This study quantifies the share of anaerobically and aerobically degradable organic matter along a transect through the Port of Hamburg, part of the tidal Elbe river (Fig. 1), and thereby provides a novel basis for future carbon budgeting studies within the investigation area. This study identifies the reactivity and size of different (kinetic) organic matter pools along the river transect based on their biodegradation rates using a three year observation period. SOM decay or SOM mineralization is defined as the amount of sediment organic carbon released by microbial decay, occurring under different environmental boundary conditions such as temperature and redox state. The latter was investigated by measuring the carbon release by microbial SOM decay under anaerobic and aerobic conditions in the laboratory. It was hypothesized that.

1. A recalcitrant (non-degradable) carbon pool can be found in the harbour sediments. This pool is larger under anaerobic conditions and smaller under aerobic conditions.
2. The input of biogenic organic matter from primary production upstream of the harbour reflects in higher SOM degradability, hence a larger pool of organic matter with high degradation rates, in upstream parts of the investigation area.
3. Downstream, a greater share of carbon is found in both, the slowly degradable and the recalcitrant organic matter pool.
4. Upper sediment layers contain more easily degradable carbon. Hence a larger share of the total carbon can be found in this labile pool.

2. Investigation area and sampling approach

Eleven locations within the tidal Elbe River around the Port of Hamburg (Fig. 1) were sampled on average every two months in the period 2018–2020, with locations P1 to P9 presenting sedimentation hotspots requiring enhanced maintenance activity by the port. At each location, between three and five sediment cores per sampling event were retrieved using a core sampler ('Frahmloot'; Shakeel et al., 2020). For each core, up to four (if present) different layers were distinguished from top to bottom: suspended particulate matter (SPM), fluid mud (FM), pre-consolidated sediment (PS), and consolidated sediment (CS). These layers were separated and a mixed sample per layer prepared from the respective material of the multiple cores. In this study, data on organic matter decay rates and organic matter pool sizes are presented for all samples from 2018 and 2019, amounting to a total of $n = 268$, extending the data set presented by Zander et al. (2020) considerably. Samples were transported to the laboratory under cool conditions in air-tight containers and processed swiftly upon arrival in the laboratory.

3. Methods

Standard sediment properties (see Table 1) were analysed according to the methods listed in Zander et al. (2020).

3.1. Anaerobic and aerobic decay of sediment organic matter

The sediment samples collected from the different layers (Section 2) were stored in their gas-tight containers the fridge at 4 °C in dark until analyses commenced, typically within a few days of sample collection. SOM decay was assessed by measuring carbon release into the gas phase (bottle headspace) over time upon incubation of the samples in the laboratory in closed glass bottles sealed with butyl rubber stoppers

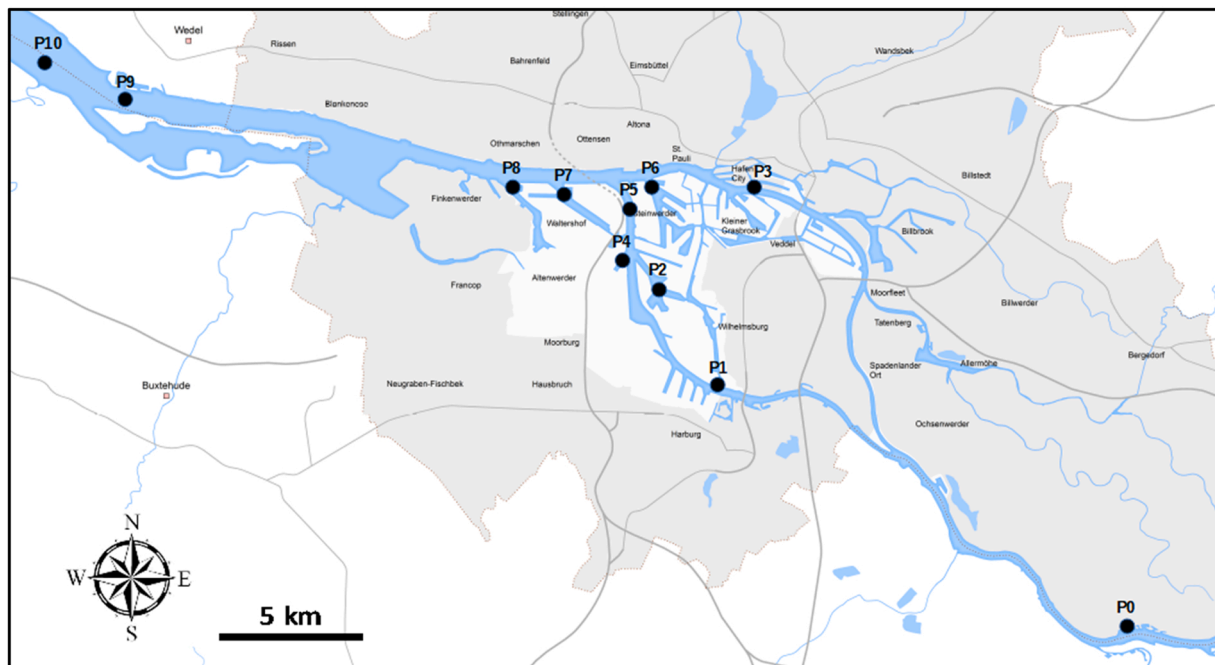


Fig. 1. Investigation area around the Port of Hamburg (adapted from Hamburg Port Authority) with sampling locations between river km 598 (P0, upstream) and 646 (P10, downstream). Further information on sampling sites and sampling strategy in Zander et al. (2020).

under anaerobic and aerobic conditions for more than 250 days (see also Zander et al., 2020). All samples were analysed in triplicate at their in situ water content.

3.1.1. Anaerobic degradation of organic matter

Depending on the water content and the expected gas production rate, about 150–300 g of fresh sample were placed into 500 ml glass bottles. The bottle headspace was flushed with 100% N₂ to establish anaerobic conditions and incubated at 36 °C in dark. The elevated experimental temperature was chosen to warrant exhaustive decay of organic matter within the time frame of the experiment (see Fig. 2) in order to assess degradability of sediment organic matter as accurately as possible.

For some samples, measurements were carried out for at least 500 days until cumulative carbon release approximated a plateau (i.e., decreased to very low rates). The total amount of generated gas was expressed as mass unit of carbon released per mass unit of organic carbon as present in the original sample. Gas chromatographic analyses did not detect any other gases besides N₂, CH₄, and CO₂. The total number of original samples analysed for anaerobic SOM degradability equalled $n = 268$.

3.1.2. Aerobic degradation of organic matter

Aerobic SOM decay was quantified at an incubation temperature of 20 °C. To determine the degradation of organic matter under aerobic (i. e., oxic) conditions, 15 g of homogenised fresh sample was incubated in 1 l glass bottles at 20 °C in the dark with a headspace of atmospheric air. The sample was distributed at the bottom of the bottles in a layer of only a few millimetres thickness in order to minimise limitations to the diffusion of oxygen into the sample.

The bottle headspace was flushed with atmospheric air in the beginning of the measurements. The generation of CO₂ was calculated from the increase in headspace CO₂ concentration, measured with gas chromatographic analyses (GC-TCD, Da Vinci Laboratory Solutions). As soon as a concentration of 2.5% CO₂ in the bottle headspace was reached, the bottle was flushed anew with atmospheric air, then measurements were resumed. Besides O₂, N₂ and CO₂, no other gases were detected. The total number of original samples analysed for aerobic SOM

degradability equalled $n = 243$ for aerobic samples.

3.1.3. Analytical details

Headspace pressure was measured manually with a pressure gauge (LEX1, Keller) using a needle pierced through the stopper. The generation of CH₄ and CO₂ (anaerobic) or only CO₂ (aerobic) was calculated from the (increase in) headspace pressure in combination with gas chromatographic analyses (GC-TCD, Da Vinci Laboratory Solutions) of headspace composition (CH₄, CO₂, O₂, N₂) using the ideal gas law. Extraction of headspace volume for GC sampling was corrected for in the calculation of gas generation and respiratory CO₂ release by measuring the headspace pressure before and after sampling. All values are reported as the sum of (CH₄-C and) CO₂-C measured in the gas phase and the share of CO₂-C dissolved in the aqueous phase. The latter was calculated using the CO₂ concentration, the volume of water, the pressure in the bottle headspace and the temperature-corrected solubility of CO₂ in water as given by Henry's constant (given in Sander, 2015). The frequency of measurements was adapted to the gas production and the respiration rates and decreased from daily intervals at the beginning of the incubation to monthly intervals at the end.

3.1.4. Incubation temperature

As decay rates are lower under anaerobic than under aerobic conditions, an elevated temperature was chosen for anaerobic incubation (36 °C versus 20 °C during aerobic incubation) to enable similar incubation time scales. The response of aerobic and anaerobic SOM decay to temperature was analysed by measuring SOM decay for > 250 days on aliquot samples incubated at 5, 10, 20, 28, 36 and 42 °C. In order to directly compare SOM decay under anaerobic and aerobic conditions, anaerobic SOM decay rates were normalised to a temperature of 20 °C based on data from this separate temperature experiment (Li, 2018). Hereby, the temperature coefficient function $Q_{16} = R_2/R_1$ was used, with R_1 and R_2 as the released carbon at the given temperature (i.e., R_1 at 20 °C and R_2 at 36 °C).

Table 1
Abiotic properties of all sediment layers and the corresponding pore water from 2018 and 2019, SD: standard deviation, TN total nitrogen, TOC total organic carbon, WC water content, Eh redox potential, LOI loss on ignition, P phosphorus, S sulphur, EC electric conductivity, DOC dissolved organic carbon, NH₄⁺ ammonium, PO₄³⁻ phosphate, Chl a chlorophyll a, Silicic acid, SO₄²⁻ sulphate. Minimum and maximum means in bold. Overall mean in italic.

	Upstream						Downstream					
	P1			P2			P3			P4		
	Mean	SD	Mean	SD	Mean	SD	Mean	SD	Mean	SD	Mean	SD
TN (%)	0.5	0.8	0.2	0.5	0.1	0.5	0.5	0.1	0.4	0.1	0.4	0.1
TOC (%)	4.0	6.4	0.8	4.2	0.5	4.2	0.6	0.5	3.1	0.9	3.7	0.3
TOC/TN (%/%)	8.6	8.1	4.3	8.3	1.1	7.8	0.6	0.5	9.2	1.7	8.3	0.2
WC (% _{DM})	387	508	276	425	369	380	286	163	341	427	300	138
Eh (mV)	-174	-212	91	-217	116	-187	174	164	-183	152	-182	166
Clay (< 2 µm, %)	38	39	9	43	8	47	5	6	31	8	42	3
Silt (2–63 µm, %)	46	52	8	50	5	47	3	5	43	9	45	3
Sand (> 63 µm, %)	16	9	7	7	5	6	3	4	26	15	13	5
LOI (%)	12	17	4	12	3	14	3	3	10	2	12	3
P (mg C/groc)	1522	2199	213	1636	179	1472	235	145	1227	204	1428	88
S (mg C/groc)	4791	4907	896	5004	1383	4967	2104	1665	4088	1325	5222	2577
pH (-)	7.3	7.3	0.2	7.5	0.2	7.6	0.2	0.2	7.6	0.2	7.5	0.2
EC (µS/cm)	1794	2147	865	1832	566	1748	445	530	1627	404	1761	596
DOC (mg/l)	27	45	66	30	28	27	18	22	22	14	23	13
NH ₄ ⁺ (mg/l)	27	100	99	21	27	18	20	21	9	11	14	12
PO ₄ ³⁻ (mg/l)	0.11	0.08	0.07	0.09	0.06	0.10	0.06	0.09	0.13	0.08	0.12	0.07
Chl a (mg/l)	19	38	27	16	11	40	21	9	19	15	14	11
Silicic acid (mg/l)	21	26	13	21	12	22	12	12	17	10	22	11
SO ₄ ²⁻ (mg/l)	81	57	52	81	57	66	60	53	88	54	69	60

3.2. Identification and quantification of differently degradable organic matter pools

The time course of cumulative carbon release was described by single phase or dual phase exponential decay functions (Eqs. 1 and 2), performed with OriginPro2019, with the choice based on the function with the higher coefficient of determination. These multi-phase models follow the same principle as the multi-G model used by Westrich and Werner (1984, reviewed by Arndt et al., 2013) for phytoplankton decay, where organic matter is split up into classes of individual compounds with separate decay rate constants (k). Dual phase first-order exponential decay functions were split into two single functions with different organic matter decay kinetics (rates) as shown in Fig. 2. The total cumulative degraded organic matter (mg C g⁻¹TOC) is the sum of the pool size of each function (y₀, Eq. 3). For each function, the organic matter decay rate (R, mg C g⁻¹TOC d⁻¹) was derived by multiplying the decay rate constant (k) and the pool size (M₀, Eq. 4). All decay rates were clustered with a k-means cluster analysis (OriginPro2019), considering the total cumulative degraded organic matter (y₀). It was used a method of vector quantization with minimum sum of squares to assign observations to groups. Observations were partitioned into clusters (k) in which each observation belongs to the cluster with the nearest mean (cluster centre). The distance between an observation and a cluster was calculated from the Euclidean distance between the observation and the cluster centre. The cut-off values separating each cluster of decay rates were used to define fast, medium and slowly degrading SOM pools (mg C g⁻¹TOC), results seen in Fig. 3. The half-lives were calculated from the time constant multiplied with the natural logarithm of two. The fourth, recalcitrant pool (not biologically available) was calculated from the difference between the total TOC concentration and the sum of pools 1–3. The recalcitrant pool was always classified as pool 4 (last pool) even when less than three pools were determined. An example for a dual rate cumulative function of fast and slow organic matter decay is shown in Fig. 2 for upstream and downstream location (P1 and P9, left and right).

$$M = -M_0 \cdot \exp(-k \cdot t) + y_0 \tag{1}$$
$$M = -M_{0a} \cdot \exp(-k_a \cdot t) - M_{0b} \cdot \exp(-k_b \cdot t) + y_0 \tag{2}$$
$$Y_0 = M_{0a} + M_{0b} \tag{3}$$
$$R = -M_0 \cdot k \tag{4}$$

with.

M₀ = total pool size of each function (a or b) in mg C g⁻¹TOC.
k = decay rate constant in d⁻¹.
t = time in days (d).
y₀ = total cumulative degraded organic matter in mg C g⁻¹TOC.
R = decay rate in mg C g⁻¹TOC d⁻¹.

4. Results

4.1. Sediment properties

Table 1 shows mean abiotic properties of all sediment layers and the corresponding pore water from 2018 and 2019. Sediments properties, methods described in Zander et al. (2020), are quite similar in the main part of the harbour (location P2 to P8). Total nitrogen, total organic carbon, silt, loss on ignition, phosphorus, pH, electric conductivity, dissolved organic matter, ammonium, phosphate and sulphate showed similar ranges in the harbour area. Clear differences are seen between the boundary locations P1 (upstream) and P9 (downstream) with highest values found at P1 for total nitrogen, total organic carbon, electrical conductivity, nutrients and silt (Table 1, bold). Location P9 reflecting the site with the highest sand content and the lowest concentration of these parameters.

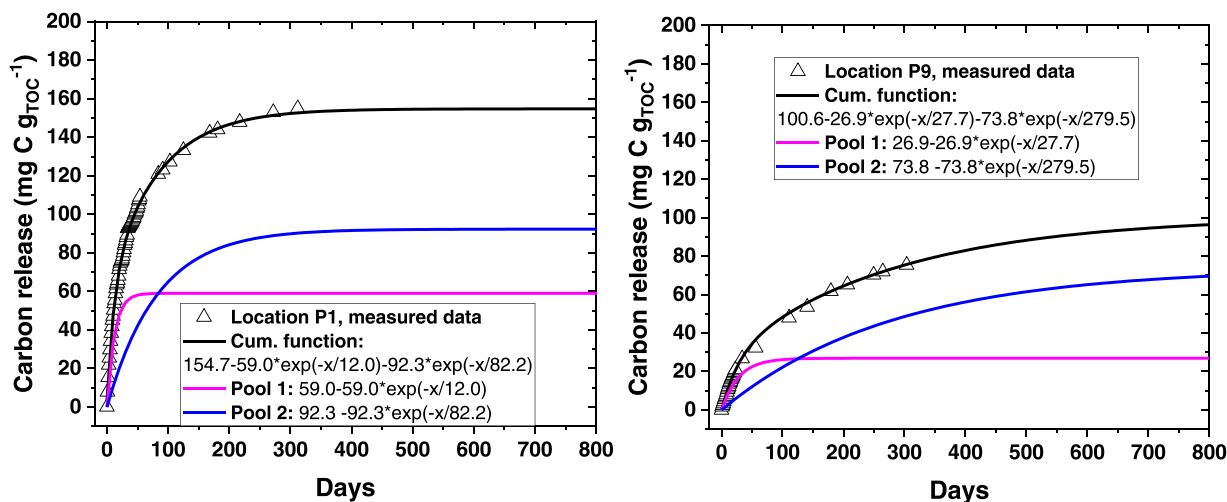


Fig. 2. Example of a dual phase cumulative function of organic matter decay with fitting functions per individual pool for upstream location P1 (left) and downstream location P9 (right) and average values of three parallels of cumulative carbon release.

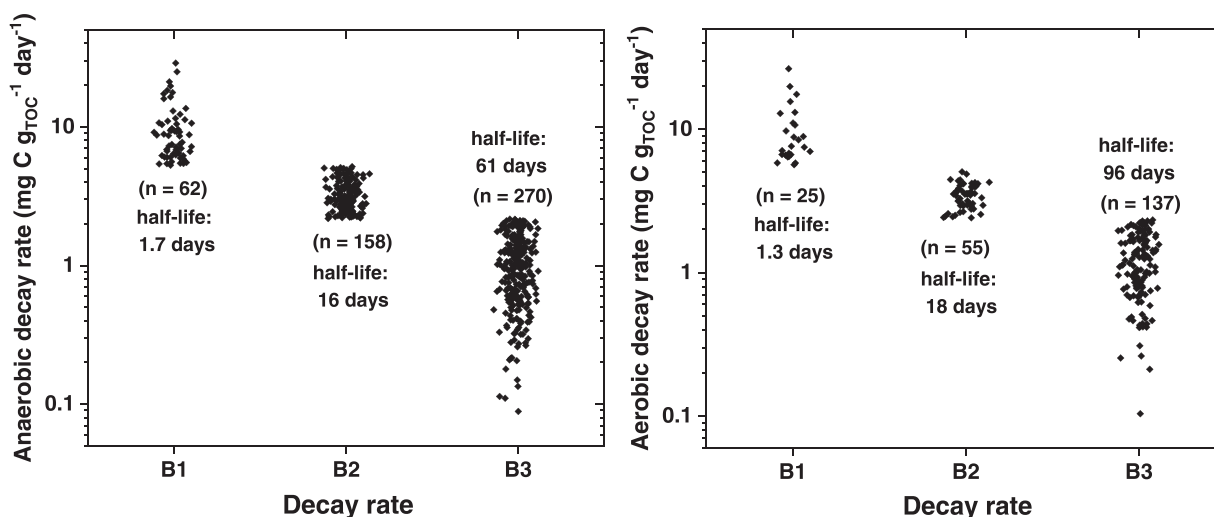


Fig. 3. Decay rates (B1, B2, B3) and averaged half-lives, of anaerobically (left) and aerobically (right) incubated samples (250 days), normalised to 20 °C, as given by the k-means cluster analysis. Samples collected from locations P1-P9 during 12 campaigns in the period 2018–2019. Sample n for aerobic decay n = 490, sample n for anaerobic decay n = 217.

4.2. Decay rates and sizes of organic matter pools

A k-means cluster analysis (see method section) was used to differentiate the data set on decay rates for anaerobic (Fig. 3, left) and aerobic SOM decay (Fig. 3, right) and to quantify the size of the according organic matter pools. It was chosen to separate three clusters with corresponding decay rates (B1, B2, B3) based on the overall range of the decay rates. The decay rates for anaerobically degrading SOM varied between 0.1 mg C g_{TOC}⁻¹ d⁻¹ and 29 mg C g_{TOC}⁻¹ d⁻¹ (Fig. 3, left) with cut-offs between pool 1 and pool 2 at 5.2 mg C g_{TOC}⁻¹ d⁻¹, and between pool 2 and pool 3 at 2.2 mg C g_{TOC}⁻¹ d⁻¹. For aerobic decay (Fig. 3, right), the range of decay rates was between 0.1 mg C g_{TOC}⁻¹ d⁻¹ and 26 mg C g_{TOC}⁻¹ d⁻¹ and the cut-off values yielded between pool 1 and pool 2 at 5.5 mg C g_{TOC}⁻¹ d⁻¹, and between pool 2 and pool 3 at 2.4 mg C g_{TOC}⁻¹ d⁻¹. Hence, both, the decay rates as well as the cut-off values to separate individual pools were very similar for anaerobic and aerobic decay. The average half-lives were between 1.7 days (B1) to 61 days (B3) for anaerobic decay (Fig. 3, left) and between 1.3 days (B1) and 96 days (B3) for aerobic decay (Fig. 3, right).

The following analyses aimed at quantifying the share of degradable

SOM under aerobic and anaerobic conditions and differentiating this share into pools characterized by different degradation kinetics. However, it is not suggested that the identified aerobically and anaerobically degradable SOM pools represent different physical entities.

Under aerobic conditions, SOM pool 1 was found mainly at upstream locations P1 and P2 (Fig. 4, top left). The size of pool 2 strongly decreased from upstream to downstream locations from around 250–50 mg C g_{TOC}⁻¹ whereas pool 3 was mostly similar along the transect, only location P1 showing slightly higher values (bottom left). For upstream locations, the total share of degradable SOM (sum of pool 1, pool 2 and pool 3) was higher than at downstream locations, as seen from the increase of the mean share of the stable pool 4 from 680 to 850 mg C g_{TOC}⁻¹ from upstream (P1) to downstream locations (P9, Fig. 4, bottom right).

Comparing aerobic and anaerobic decay conditions, aerobic decay showed a larger share of degradable organic matter (Figs. 4 and 5, sum of pool 1, pool 2 and pool 3). The aerobic decay exceeding the anaerobically degradable share by around 100 mg C g_{TOC}⁻¹ at location P1. At downstream location P9, the anaerobically and aerobically degradable share was about equal.

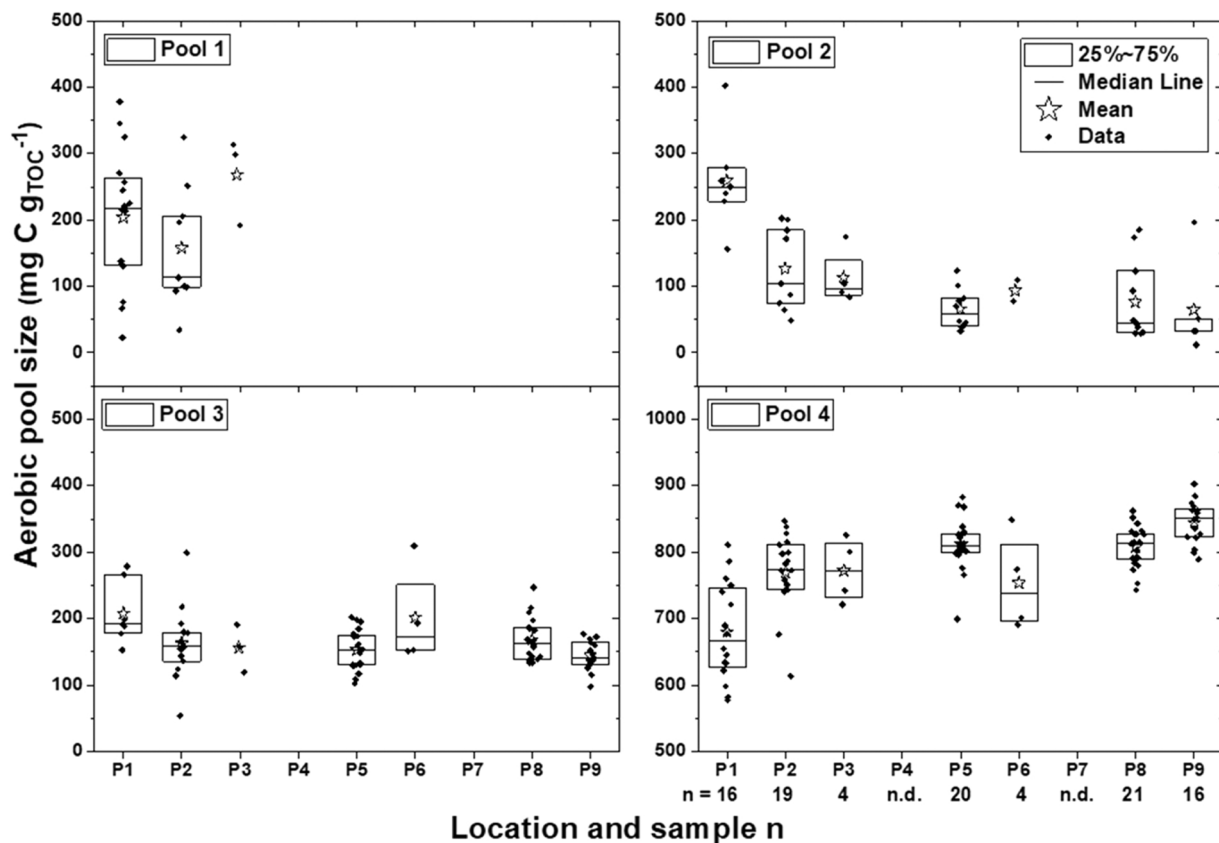


Fig. 4. Size of aerobically degradable SOM pools ($\text{mg C g}_{\text{TOC}}^{-1}$) per location for four pools and all layers, samples taken in 2018 and 2019. Consider the differently scaled y-axis for the non-degradable pool 4 (bottom right). Lines = median values, stars = mean values, boxes = 25th and 75th percentile, n.d. = not determined. The sample n is valid for pool 4, because not all pools appeared for each sample.

Under anaerobic conditions, samples with the most rapidly degrading SOM pool 1, corresponding to decay rate B1, were found mainly at upstream locations P1 and P2 (Fig. 5, top left). The largest size of pool 2 was at P5 and P9 (Fig. 5, top right). The size of pool 3 was mostly similar along the transect, slightly decreasing from upstream to downstream (bottom left). At upstream location P1, the total share of degradable SOM (sum of carbon in pools 1–3) was higher than at intermediate and downstream locations. This was indicated by the significantly (non-paired t-test: 0.0003) lower amount of carbon in the non-degradable (stable) pool 4 (Fig. 5, bottom right). At upstream location P1, 240 $\text{mg C g}_{\text{TOC}}^{-1}$ were anaerobically degradable (760 $\text{mg C g}_{\text{TOC}}^{-1}$ non-degradable) whereas at downstream location P9, only 160 $\text{mg C g}_{\text{TOC}}^{-1}$ were anaerobically degradable (840 $\text{mg C g}_{\text{TOC}}^{-1}$ non-degradable).

In terms of depth profiles, fluid mud (FM) on average had a share of around 39% (anaerobic conditions, Fig. 6, left) and 34% (aerobic conditions, Fig. 6, right) of degradable carbon (i.e., the sum of pool 1, pool 2 and pool 3), whereas consolidated sediment (CS) harboured 28% of anaerobically and 30% of aerobically degradable carbon (Fig. 6). For anaerobic decay (Fig. 6, left), the share of pool 1 and pool 2 was largest for FM layers, pool 4 increased with depth (FM to CS) from 61% to 72%. For aerobically degradable SOM pools (Fig. 6, right), no pool 1 was observed for CS layers, depth related trends were less pronounced than for anaerobic SOM pools. The initial average TOC content was 3.9% for FM and pre-consolidated sediment (PS) layers and 3.7% for CS layers.

Location P1 is the least disturbed location in the Port of Hamburg in terms of dredging and was therefore considered the best choice to investigate time and depth-related trends. Redox potentials revealed mostly anaerobic conditions in the sediment package. Hence, Fig. 7 focusses on the time- and depth-related trends for anaerobic SOM decay at location P1. A clear seasonal trend was observed for the size of the easily degradable pool 1. The size of pool 1 increased from 45 $\text{mg C g}_{\text{TOC}}^{-1}$

in March to 220 $\text{mg C g}_{\text{TOC}}^{-1}$ in June, followed by a decrease towards the end of the year (Fig. 7, left). This trend was less pronounced at other locations and not detectable in other pools. The average pool sizes decreased with depth (SPM to CS layer) for pool 1 and pool 2 (Fig. 7, right). For pool 1 and pool 2, the degradable SOM was mainly found in SPM and PS layers (Fig. 7, right) whereas pool 3 showed similar pool sizes for all layers.

5. Discussion

5.1. Spatial trends of sediment organic matter (SOM) degradable pools

Organic matter can be viewed as a continuum of successively degrading compounds (Lehman and Kleber, 2015), each with their individual decay constant (Boudreau and Ruddick, 1991). This study attempts to cluster this succession of degradability in freshwater sediments of the Elbe river by separating a fast (P1), medium (P2) and slowly (P3) degradable organic matter pool. The degradability was characterised by discrete first order rate constants, with half-lives of hours to days, days to weeks and weeks to months (Fig. 3). This attempt was similar to the work of Westrich and Berner (1984), also reviewed by Arndt et al. (2013). It was assumed that the decay rates of easily degradable (i.e., freshly settled riverine organic matter) are high and decay rates of older (i.e., more mineral-bound, physically protected organic matter) are low (Rothman and Forney, 2007). The decay rates derived from the rate constants k were used to define and quantify the differently degradable organic matter pools. A recalcitrant pool 4, which was considered not biologically available, was calculated from the difference between the total TOC concentration and the sum of pools 1–3.

The recalcitrant average share ranged mostly between 65 % and 85 % (aerobic conditions, Fig. 4, bottom right) and 75–85 % of TOC

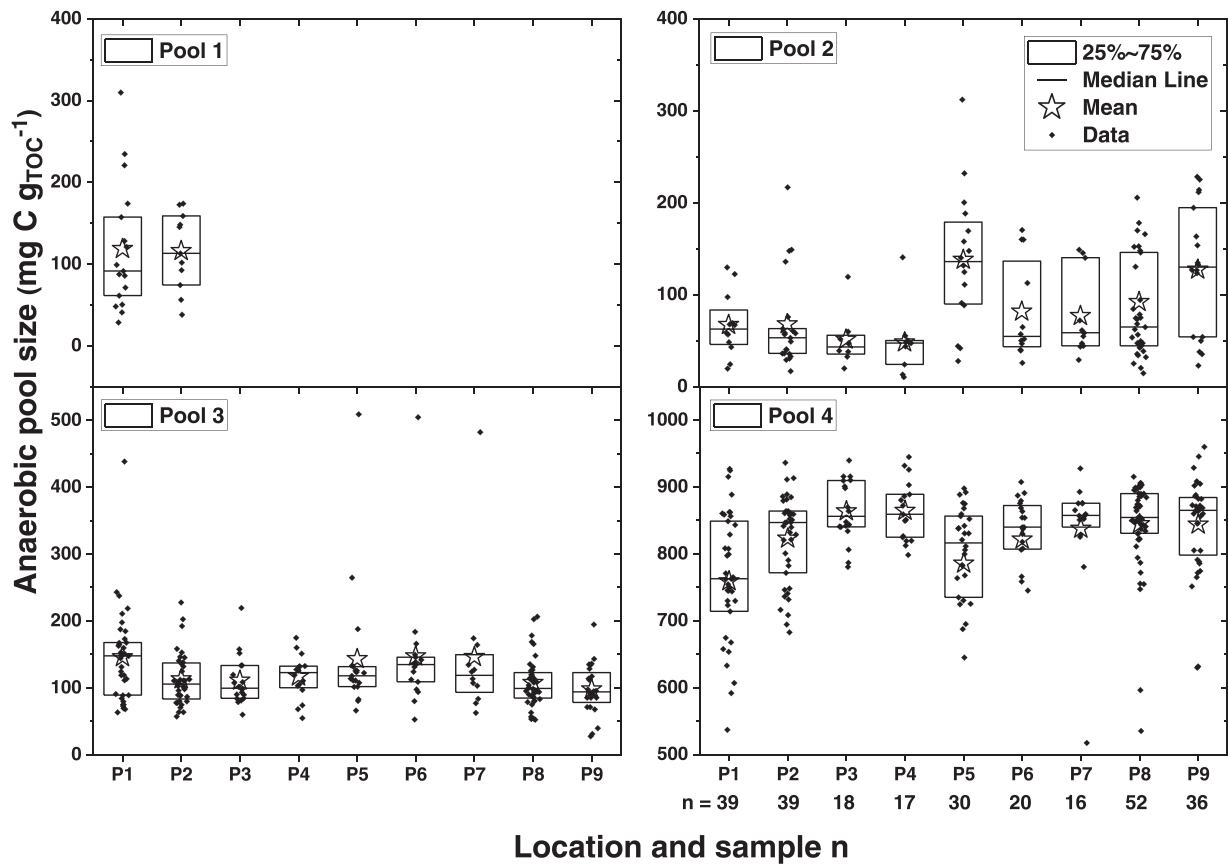


Fig. 5. Size of anaerobically degradable SOM pools (mg C gTOC⁻¹) per location for four pools and all layers, samples taken in 2018 and 2019. Consider the differently scaled y-axis for the non-degradable pool 4 (bottom right). Lines = median values, stars = mean values, boxes = 25th and 75th percentile. The sample n is valid for pool 4, because not all pools appeared for each sample.

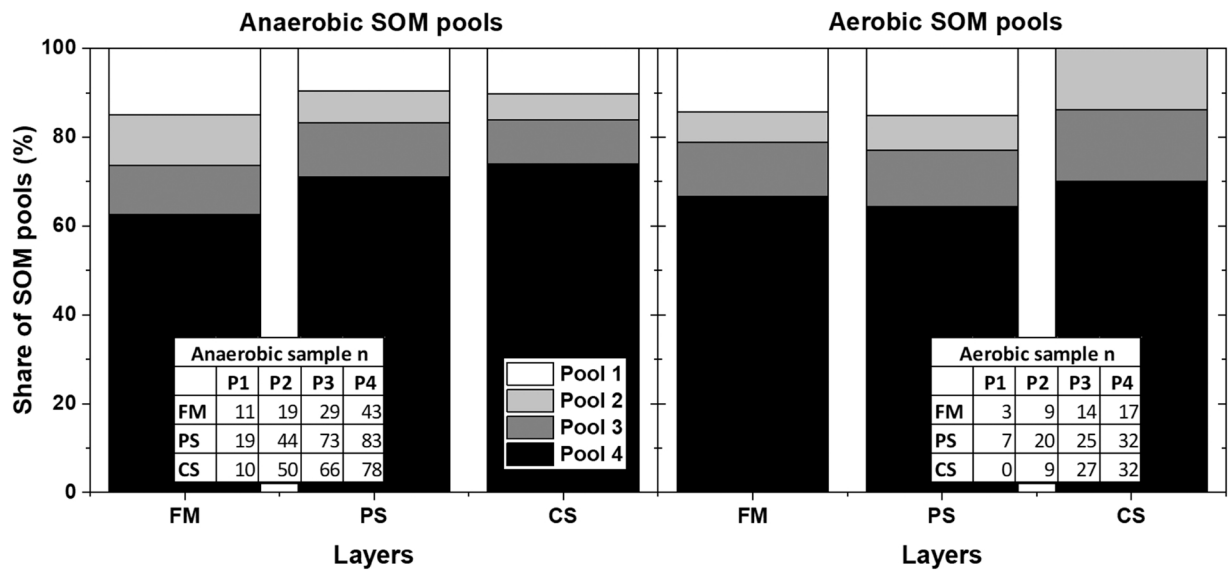


Fig. 6. Relative share of the four sediment organic matter pools (pool 1–4) per layer (FM, PS, CS) from all locations, samples from 2018 and 2019. Left: anaerobically degraded SOM pools, right: aerobically degraded SOM pools.

(anaerobic conditions, Fig. 5, bottom right). This indicated that in most samples the greatest part of SOM was stable and not available to microbial decay. On average, about 10% more SOM was degradable when oxygen was available as terminal electron acceptor. This could be explained by the more favourable thermodynamics with the larger

energy gain of the aerobic degradation pathway and the fact that under anaerobic conditions hydrolysis and fermentation of structurally complex organic matter are rate-limiting (Kristensen, 1995). Complete mineralization as well as degradation of larger molecules (i.e., lignin) is only accomplished under aerobic conditions. Further, estrogens,

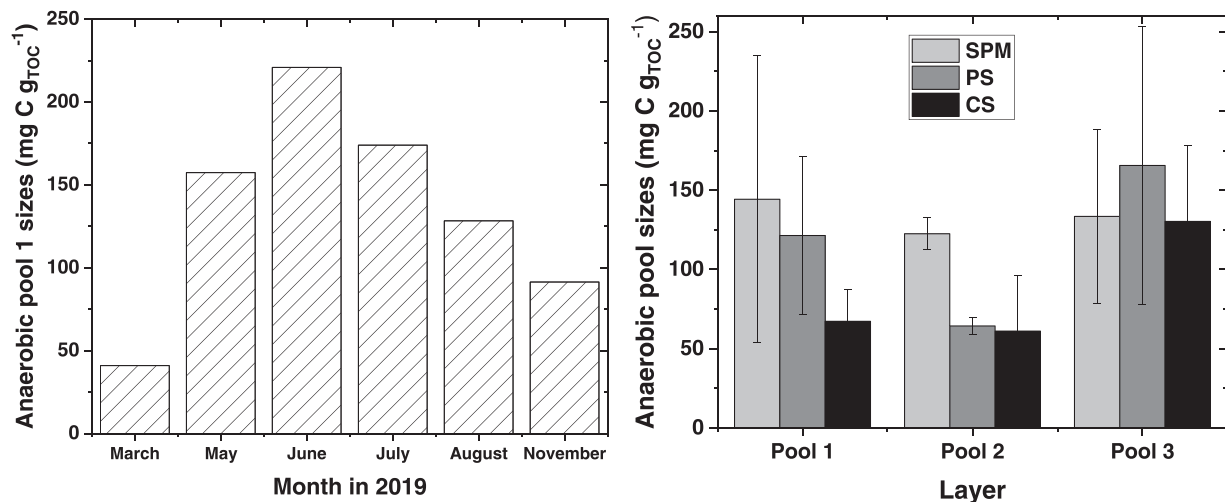


Fig. 7. The anaerobically degradable pool 1 from March to November 2019 (left) and average ($n = 12$, 2018 and 2019) anaerobic pool sizes for SPM, PS and CS layers for pool 1, pool 2 and pool 3 (right), both at location P1.

phthalates and surfactants are rapidly decomposed under aerobic conditions (Blume et al., 2016) but not under anaerobic conditions. Correspondingly, the recalcitrant pool 4 was larger under anaerobic conditions. At upstream location P1, largest differences between aerobic and anaerobic decay was found for pool 1 and pool 2. From upstream to downstream, the differences between aerobic and anaerobic pool sizes decreased. In an earlier study on dewatered and recently landfilled dredged sediment from the Port of Hamburg, the anaerobically degradable share amounted to only 3–11 % of the organic carbon (Gebert et al., 2019). Hence a higher share of up to 89–97 % of TOC to be present in the recalcitrant pool. It is plausible that for the dewatered and landfilled sediment the degradable SOM fraction is smaller than for the freshly sampled sediment analysed in this study. Pre-treatment and several years of landfilling will have led to further depletion of degradable SOM under first aerobic (during dewatering) and subsequently under anaerobic (landfilling) conditions.

The apparent lack of an aerobically and aerobically degradable pool 1 at downstream locations (Fig. 4, top left) was interpreted as a successive depletion of easily degradable organic matter as the sediment passes through the harbour area. This could be explained by the correspondingly larger share of easily degradable organic matter at location P1. A strong decrease in the aerobically available pool 2 was observed along the transect (Fig. 4, top right), mirrored by an increase in the recalcitrant pool 4 (Fig. 4, bottom right). Both under aerobic and under anaerobic conditions, the size of the slowly degradable pool 3 did not show a spatial gradient (Figs. 4 and 5, bottom left). It is hypothesised that this pool constitutes a basis of about 150–200 mg C g_{TOC}⁻¹ (aerobic conditions, 15–20% of TOC) and 100–150 mg C g_{TOC}⁻¹ (anaerobic conditions, 10–15 % of TOC) of mineral-bound slowly degradable SOM of predominantly downstream origin at all sampling locations. This pool does not contribute significantly to carbon release in the short or intermediate time scales when sediment is naturally transported from upstream to downstream.

About half of the high anaerobic and aerobic decay rates (B1, Fig. 3, left and right) were found at location P1, reflecting the dominance of the easily degradable organic matter (pool 1) at upstream locations (Fig. 5, top left), resulting from the upstream input of biomass. Correspondingly, the recalcitrant pool 4 was smaller by approximately 100 mg C g_{TOC}⁻¹ at upstream location P1 compared to location P9 (Fig. 5 and Fig. 4, bottom right). The largest share of the mineral bound organic matter reaches the harbour from downstream with the tide. This was indicated by the concentration of Zn in the particle size fraction < 20 µm (Kappenberg and Fanger, 2007), showing elevated concentrations and therefore an upstream signature only at locations P0 and P1 (Table 1). Reese et al.

(2019) clustered sediment of the Elbe River as fluvial (to river km 615) and as a mixture of marine and fluvial (between river km 615 and 700). They based their clusters on element fingerprinting and isotopic tracer approaches. These findings are corroborated by higher upstream oxygen consumption rates (Spieckermann et al., 2021) and higher upstream shares of organic carbon bound in the low density fraction and lower $\delta^{13}\text{C}$ values (Zander et al., 2020). Further it was indicated by increased values of parameters representing phytoplankton biomass such as chlorophyll a and silicic acid (Table 1). Also, increased concentrations of solid phase nutrients (phosphorus, sulphur, nitrogen) and carbon were found at upstream location P1. Hence, the spatial patterns of SOM degradability found in this study are directly linked to source gradients of labile autochthonous planktonic biomass, adding a small, but very reactive organic matter fraction of upstream origin to the larger part of recalcitrant organic matter from downstream.

5.2. Organic matter decay rates and degradable shares in soils and sediments

In this section, comparisons of decay rates and SOM pool sizes with literature will be made, including data from terrestrial soils. It is evident that organic matter decay in soils is governed by different environmental conditions (i.e., degree of saturation, redox potential, temperature) and different sources of organic matter input. However, both, terrestrial soils and sediments, comprise older, mature organic matter stabilized in organo-mineral complexes as well as fresh, immature and easily degradable organic matter originating from microbial, plant or animal biomass. Moreover, sediment organic matter also comprises eroded topsoil organic matter, while terrestrial soils in the river catchment originate from river deposits during flooding.

For various terrestrial soils, Haynes (2005) listed values of potentially degradable carbon for soils between 0.8 % and 12 % of TOC, mostly between 5 % and 15 % of TOC. The sediments of this study showed, compared to Haynes (2005), higher values of degradable organic matter under anaerobic conditions, namely, on average between 13 % and 23 % of TOC (compare values for the recalcitrant pool 4, Fig. 5). A higher share of degradable organic matter can be explained by the continuous input of young, biogenic (phytoplankton), and less degraded sediment-bound organic matter, reaching the investigation area from the upstream parts of the river (Schoel et al., 2014). The input of phytoplankton adds an organic matter pool with an elevated degradable share of up to 50 % (e.g. Westrich and Berner, 1984). In soils, high decay rates are associated with microbial biomass and are typically found in the lighter density fraction Von Lützow et al. (2007). In

agreement with findings from McKew et al. (2013), the rates of carbon release by microbial decay of sediment organic matter were similar under aerobic and anaerobic conditions (Fig. 3).

In this study, the mean residence times (MRT) for degradable sediment organic matter (not shown) varied between three to five years if decay rates were normalised to 20 °C and between 30 and 40 years if decay rates were normalized to 10 °C. In comparison, MRT are given with 30–87 years for soils under corn cultivation (Schiedung et al., 2017) and with 10–30 years for forest soils (temperatures between 7 °C and 13 °C, Garten and Hanson, 2006). Oades (1988) mentioned MRT between 4 and 200 years for various soils. The higher MRT found for sediment organic matter in this study plausibly indicates the presence of younger, more easily degradable organic matter (i.e., phytoplankton with low MRT) when compared to the MRT of the already partly mineralized older organic matter of terrestrial soils mentioned above. Further, the MRT of this study (3–5 years, 20 °C) grouped within order of magnitude of the half-life (2.5 ± 4.7 years) of organic matter previously measured for inland waters (Catalán et al., 2016, 20 °C). Similarly, the values for the decay rate constants k_1 and k_2 for aerobic SOM decay (data not shown), derived from the multi-phase first order exponential fitting of the carbon release over time (Fig. 2) and used to calculate SOM degradation rates (Eq. 4, Fig. 3), are very similar to those previously reported for several studies on oxic phytoplankton composition by Westrich and Berner (1984). This corroborates the assumption that the degradability of organic matter is driven by the concentration of phytoplankton-derived labile organic matter present in the composite sediment in addition to the slowly degradable pool 3, comprising the organic matter fraction stabilized in organo-mineral complexes.

5.3. Trends in time and with depth

In the investigated harbour area, sedimentation dynamics are influenced by maintenance dredging, disturbing the natural development of sediment depth profiles. Therefore, depth-related assumptions are made with reservation. Examples of depth-related patterns for various sediment parameters (i.e., SOM decay, carbon stable isotopes, DNA in extrapolymeric substances, pore water NH_4^+ concentration) were given in Zander et al. (2020). It was assumed that decreasing trends of observed SOM decay (rates) with depth are due to decreasing degradability of in situ SOM in older (deeper) sediment layers. This assumption was supported by the share of organic matter in differently degradable pools (Fig. 6, left). Under anaerobic conditions, the largest share of degradable carbon was found in the fluid mud samples, decreasing with depth and hence age of the sediment. Therefore it was assumed that due to carbon decay, occurring in situ before sediment sampling, the share of degradable carbon is lower at depth. The depth gradient clearly showed larger shares of easily degradable SOM in upper layers (SPM and PS) and more decayed SOM in deeper layers (CS). This was true for the more easily degradable pools 1 and 2 (Fig. 7, right). Increased pool 1 sizes (Fig. 7, left) between spring and summer indicated an upstream growth of phytoplankton (Deng et al., 2019; Schoel et al., 2014). Similarly, Grossart et al. (2004) found seasonal patterns in a tidal flat ecosystem, namely, high sediment resuspension in November and phytoplankton-related processes influencing bacterial dynamics in May. Subsequent input of fresh organic matter at upstream locations (P1) was also indicated by increased chlorophyll *a* and silicic acid concentrations at location P1 (Table 1). This was supported by a diminishing share of easily degradable SOM between summer and autumn, in other words, a decreasing pool 1 in the second part of the year. It was assumed that the input of fresh SOM in March from upstream was still low due to high winter discharge, in combination with still low irradiation (Kamjunke et al., 2021), low water and sediment temperatures. A similar seasonal pattern was also described for the sediment oxygen consumption potential in the investigation area (Spieckermann et al., 2021) with highest oxygen consumption values for the summer months due to a larger of easily degradable biomass. Independent of this seasonally varying input

of phytoplankton-derived, easily degradable organic matter, SOM mineralization rates are strongly controlled by in situ temperature, as also shown by Gudas et al. (2010) for sediments of boreal lakes.

6. Conclusions and outlook

This paper provides quantitative data on the total mass of carbon that can be released from microbial mineralization of organic matter in freshwater tidal sediments, quantifies pools of different organic matter lability and provides the corresponding degradation rates. SOM lability along a transect of 30 river kilometres though the Elbe around the Port of Hamburg decreased from upstream to downstream, evidenced by the decreasing amount of the easily degradable pool 1 material from upstream to downstream. The slowly degradable pool 3 is assumed to be associated with SOM bound in organo-mineral complexes. Pool 3 is spread more or less equally along the investigated transect, constituting a similar share of predominantly marine origin at all locations. Total degradability thus appears to be governed by the amount of reactive SOM present in addition to this basis (pool 1, 10–15% and pool 2, 5–10%), which in turn follows a source gradient and an age gradient from upstream to downstream. The recalcitrant pool 4 comprised by far the largest part of TOC in any part of the harbour, indicating that for both, anaerobic and aerobic conditions, the sediment organic matter for the largest part is stable. The sediments therefore contribute significantly to organic carbon storage in the investigation area. The size of the anaerobically degradable SOM pools decreased with depth and hence age of organic matter and varied seasonally in relation to the variability of upstream net primary production. Total SOM degradability was larger under aerobic than under anaerobic conditions by about 10% of TOC but the differences between aerobic and anaerobic decay decreased from upstream to downstream. The upper sediment layers, characterised by the highest amount of young organic matter, still showed a large share of poorly degradable and recalcitrant SOM (pools 3 and 4). This suggests that in the investigated system organic matter, even in the suspended and fluidic particle phases, is already significantly degraded or stabilized in organo-mineral associations. The size of the differently degradable organic matter pools and the degradation rates can be used to quantify carbon fluxes from microbial decay of sediment organic matter in the tidal Elbe river, using data on in situ temperatures and the known temperature dependency of anaerobic and aerobic decay.

CRedit authorship contribution statement

Florian Zander carried out the experiments, processed the experimental data, performed the analysis, drafted the manuscript and designed the figures with support from Julia Gebert. Alexander Gröngroft and Timo J. Heimovaara provided valuable feedback to the analytical concept. Annette Eschenbach and Timo J. Heimovaara contributed to the final version of the manuscript. All authors provided critical feedback and helped shape the manuscript. Julia Gebert supervised the project.

Declaration of Competing Interest

The authors declare that they have no known competing financial interests or personal relationships that could have appeared to influence the work reported in this paper.

Acknowledgements

This study was funded by Hamburg Port Authority and carried out within the project BIOMUD, a member of the MUDNET academic network www.tudelft.nl/mudnet/.

References

- Arndt, S.B., Jørgensen, B.B., LaRowe, D.E., Middelburg, J.J., Pancost, R.D., Regnier, P., 2013. Quantifying the degradation of organic matter in marine sediments: a review and synthesis. *Earth Sci. Rev.* 123, 53–58. <https://doi.org/10.1016/j.earscirev.2013.02.008>.
- Baldock, J.A., Skjemstad, J.O., 2000. Role of the soil matrix and minerals in protecting natural organic materials against biological attack. *Org. Geochem.* 31, 697–710. [https://doi.org/10.1016/S0146-6380\(00\)00049-8](https://doi.org/10.1016/S0146-6380(00)00049-8).
- Blume, H.P., Brümmner, G.W., Fleige, H., Horn, R., Kandeler, E., Kögel-Knabner, I., Kretzschmar, R., Stahr, K., Wilke, B.-M., Scheffer, F., Schachtschabel, P., 2016. *Soil Science*. Berlin Heidelberg Springer-Verlag. <https://doi.org/10.1007/978-3-642-30942-7>.
- Boudreau, B.P., Ruddick, B.R., 1991. On a rective continuum of organic matter diagenesis. *Am. J. Sci.* 291, 507–538.
- Boyd, A.McKew, Dumbrell, A.J., Taylor, J.D., McGenity, T.J., Underwood, G.J.C., 2013. Differences between aerobic and anaerobic degradation of microphytobenthic biofilm-derived organic matter within intertidal sediments. *FEMS Microbiol. Ecol.* 84 (3), 495–509. <https://doi.org/10.1111/1574-6941.12077>.
- Brockmann, U.H., 1994. Organic matter in the Elbe Estuary. *Neth. J. Aquat. Ecol.* 28 (3–4), 371–381. <https://doi.org/10.1007/BF02334207>.
- Burdige, D.J., 2007. Preservation of organic matter in marine sediments: controls, mechanisms and an imbalance in sediment carbon budgets? *Chem. Rev.* 107, 467–785.
- Catalán, N., Marcé, R., Kothawala, D.N., Tranvik, L.J., 2016. Organic carbon decomposition rates controlled by water retention time across inland waters. *Nat. Geosci.* 9. <https://doi.org/10.1038/NGEO2720>.
- Deng, Z., He, Q., Safar, Z., Chassagne, C., 2019. The role of algae in fine sediment flocculation: In-situ and laboratory measurements. *Mar. Geol.* 413, 71–84. <https://doi.org/10.1016/j.margeo.2019.02.003>.
- Gao, J., Mikutta, R., Jansen, B., Guggenberger, G., Vogel, C., Kalbitz, K., 2019. The multilayer model of soil mineral–organic interfaces—a review. *J. Plant Nutr. Soil Sci.* 183, 27–41. <https://doi.org/10.1002/jpln.201900530>.
- Garten, C.T., Hanson, P.J., 2006. Measured forest soil C stocks and estimated turnover times along an elevation gradient. *Geoderma* 136, 342–352. <https://doi.org/10.1016/j.geoderma.2006.03.049>.
- Gebert, J., Knoblauch, C., Gröngroft, A., 2019. Gas production from dredged sediment. *Waste Manag.* 85, 82–89. <https://doi.org/10.1016/j.wasman.2018.12.009>.
- Geerts, L., Cox, T.J.S., Maris, T., Wolfstein, K., Meire, P., Soetaert, K., 2017. Substrate origin and morphology differentially determine oxygen dynamics in two major European estuaries, the Elbe and the Schelde. *Estuar. Coast. Shelf Sci.* 191, 157–170. <https://doi.org/10.1016/j.ecss.2017.04.009>.
- Grasset, C., Mendonça, R., Saucedo, G.V., Bastviken, D., Roland, F., Sobek, S., 2018. Large but variable methane production in anoxic freshwater sediment upon addition of allochthonous and autochthonous organic matter. *Limnol. Oceanogr.* 63, 1488–1501. <https://doi.org/10.1002/lno.10786>.
- Grasset, S., Moras, S., Isidorova, A., Couture, R.-M., Linkhorst, A., Sobek, S., 2021. An empirical model to predict methane production in inland water sediment from particular organic matter supply and reactivity. *Limnol. Oceanogr.* 9999 (2021), 1–13. <https://doi.org/10.1002/lno.11905>.
- Grossart, H.-P., Brinkhoff, T., Martens, T., Dierselen, C., 2004. Tidal dynamics of dissolved and particulate matter and bacteria in a tidal flat ecosystem in spring and fall. *Limnol. Oceanogr.* 49 (6), 2212–2222. <https://doi.org/10.4319/lno.2004.49.6.2212>.
- Gudasz, C., Bastviken, D., Steger, K., Premke, K., Sobek, S., Tranvik, L.J., 2010. Temperature-controlled organic carbon mineralization in lake sediments. *Nature* 466, 478–482. <https://doi.org/10.1038/nature093>.
- Haynes, R.J., 2005. Labile organic matter fractions as central components of the quality of agricultural soils: an overview. *Adv. Agron.* 85, 221–268.
- Jommi, C., Muraro, S., Trivellato, E., Zwaneburg, C., 2019. Experimental results on the influence of gas on the mechanical response of peats. *Géotechnique* 69 (9), 753–766. <https://doi.org/10.1680/jgeot.17.P.148>.
- Jørgensen, B.B., 1979. A comparison of methods for the quantification of bacterial sulfate reduction in coastal marine sediments II. *Calc. Math. Models Geomicrobiol.* 1, 29–47. <https://doi.org/10.1080/01490457809377722>.
- Jørgensen, B.B., 1982. Mineralization of organic matter in the sea bed -The role of sulphate reduction. *Nature* 296, 643–645.
- Kamjunke, N., Rode, M., Baborowski, M., Kunz, J.V., Zehner, J., Borchardt, D., Weitere, M., 2021. High irradiation and low discharge promote the dominant role of phytoplankton in riverine nutrient dynamics. *Limnol. Oceanogr.* 66, 2648–2660. <https://doi.org/10.1002/lno.11778>.
- Kappenberg, J., Fanger, H.-U., 2007. Sedimenttransportgeschehen in der tidebeeinflussten Elbe, der Deutschen Bucht und in der Nordsee. GKSS report 2007/20, ISSN 0344–9629.
- Kristensen, E., 1995. Aerobic and anaerobic decomposition of organic matter in marine sediment: which is fastest? *Limnol. Oceanogr.* 40, 1430–1437. <https://doi.org/10.4319/lno.1995.40.8.1430>.
- Lehman, J., Kleber, M., 2015. The contentious nature of soil organic matter. *Nature* 528, 60–68. <https://doi.org/10.1038/nature16069>.
- Li, X., 2018. Investigation of Gas Generation by Riverine Sediments: Production Dynamics and Effects of Sediment Properties (M.Sc. thesis). Delft University of Technology.
- Malarkey, J., Baas, J.H., Hope, J.A., Aspdren, R.J., Parsons, D.R., Peakall, J., Paterson, D.M., Schindler, R.J., Ye, L., Lichtman, I.D., Bass, S.J., Davies, A.G., Manning, A.J., Thorne, P.D., 2015. The pervasive role of biological cohesion in bedform development. *Nat. Commun.* 6, 6257. <https://doi.org/10.1038/ncomms7257>.
- McKew, B.A., Dumbrell, A.J., Taylor, J.D., McGenity, T.J., Underwood, G.J.C., 2013. Differences between aerobic and anaerobic degradation of microphytobenthic biofilm-derived organic matter within intertidal sediments. 495–50 FEMS Microbiol. Ecol. 84. <https://doi.org/10.1111/1574-6941.12077>.
- Middelburg, J.J., 1989. A simple rate model for organic matter decomposition in marine sediments. *Geochim. Cosmochim. Acta* 53, 1577–1581.
- Middelburg, J.J., Meysman, F.J.R., 2007. Burial at sea. *Science* 316, 1294–1295. <https://doi.org/10.1126/science.1144001>.
- Oades, J.M., 1988. The retention of organic matter in soils. *Biogeochem* 5, 35–70. <https://doi.org/10.1007/BF02180317>.
- Parsons, D.R., Schindler, R.J., Hope, J.A., Malarkey, J., Baas, J.H., Peakall, J., Manning, A.J., Ye, L., Simmons, S., Paterson, D.M., Aspdren, R.J., Bass, S.J., Davies, A.G., Lichtman, I.D., Thorne, P.D., 2016. The role of biophysical cohesion on subaqueous bed form size. *Geophys. Res. Lett.* 43, 1566–1573. <https://doi.org/10.1002/2016GL067667>.
- Rabalais, N.N., Diaz, R.J., Levin, L.A., Turner, R.E., Gilbert, D., Zhang, J., 2010. Dynamics and distribution of natural and human-caused hypoxia. *Biogeosciences* 7, 585–619. <https://doi.org/10.5194/bg-7-585-2010>.
- Rothman, D.H., Forney, D.C., 2007. Physical model for the decay and preservation of marine organic carbon. *Science* 316, 1325–1328.
- Sander, R., 2015. Compilation of Henry's law constants (version 4.0) for water as solvent. *Atmos. Chem. Phys.* 15, 4399–4981. <https://doi.org/10.5194/acp-15-4399-2015>.
- Schiedung, H., Tilly, N., Hütt, C., Welp, G., Brüggemann, N., Amelung, W., 2017. Spatial controls of topsoil and subsoil organic carbon turnover under C3–C4 vegetation change. *Geoderma* 303, 44–51. <https://doi.org/10.1016/j.geoderma.2017.05.006>.
- Schoel, A., Hein, B., Wyrwa, J., Kirchesch, V., 2014. Modelling water quality in the Elbe and its estuary—large scale and long term applications with focus on the oxygen budget of the estuary. *Die Kueste* 81, 203–232.
- Shakeel, A., Kirichek, A., Chassagne, C., 2019. Is density enough to predict the rheology of natural sediments? *Geo Mar. Lett.* 39, 427–434. <https://doi.org/10.1007/s00367-019-00601-2>.
- Shakeel, A., Kirichek, A., Chassagne, C., 2020. Rheological analysis of natural and diluted mud suspensions. *J. Non-Newton. Fluid* 286, 104434. <https://doi.org/10.1016/j.jnnfm.2020.104434>.
- Shakeel, A., Zander, F., de Kerk, J.-W., Kirichek, A., Gebert, J., Chassagne, C., 2022. Effect of organic matter degradation in cohesive sediment: A detailed rheological analysis. *J. Soil Sediment.* <https://doi.org/10.1007/s11368-022-03156-5>.
- Sills, G.C., Gonzalez, R., 2001. Consolidation of naturally gassy soft soil. *Geotechnique* 51 (7), 629–639. <https://doi.org/10.1680/geot.2001.51.7.629>.
- Six, J., Paustian, K., 2014. Aggregate-associated soil organic matter as an ecosystem property and a measurement tool. *Soil Biol. Biochem.* 68, A4–A9. <https://doi.org/10.1016/j.soilbio.2013.06.014>.
- Spieckermann, M., Gröngroft, A., Karrasch, M., Neumann, A., Eschenbach, A., 2021. Oxygen consumption of resuspended sediments of the upper elbe estuary: process identification and prognosis. *Aquat. Geochem.* <https://doi.org/10.1007/s10498-021-09401-6>.
- Tillmann, U., Hesse, K.-J., Colijn, F., 2000. Planktonic primary production in the German Wadden Sea. *J. Plankton Res.* 22, 1253–1276. <https://doi.org/10.1093/plankt/22.7.1253>.
- van Duyl, F.C., de Winder, B., Kop, A.J., Wollenzien, U., 1999. Tidal coupling between carbohydrate concentrations and bacterial activities in diatom-inhabited intertidal mudflats. *Mar. Ecol. Prog. Ser.* 191, 19–32. <https://doi.org/10.3354/meps191019>.
- Von Lütow, M., Koegel-Knabner, I., Ekschmitt, K., Flessa, H., Guggenberger, G., Matzner, E., Marschner, B., 2007. SOM fractionation methods: relevance to functional pools and to stabilization mechanisms. *Soil Biol. Biochem.* 39, 2183–2207. <https://doi.org/10.1016/j.soilbio.2007.03.007>.
- Ward, N.D., Krusche, A.V., Sawakuchi, H.O., Brito, D.C., Cunha, A.C., Moura, J.M.S., da Silva, R., Yager, P.L., Keil, R.G., Richey, J.E., 2015. The compositional evolution of dissolved and particulate organic matter along the lower Amazon River—Obidos to the ocean. *Mar. Chem.* 177, 244–256. <https://doi.org/10.1016/j.marchem.2015.06.013>.
- Westrich, J.T., Berner, R.A., 1984. The role of sedimentary organic matter in bacterial sulfate reduction: the G model tested. *Limnol. Oceanogr.* 29 (2), 236–249.
- Wolfstein, K., Kies, L., 1999. Composition of suspended particulate matter in the Elbe estuary: implications for biological and transportation processes. *Dtsch. Hydrogr. Z.* 51 (4), 453–463. <https://doi.org/10.1007/BF02764166>.
- Wolfstein, K., Colijn, F., Doerffer, R., 2000. Seasonal dynamics of microphytobenthos biomass and photosynthetic characteristics in the northern German Wadden Sea, obtained by the photosynthetic light dispensation system. *Estuar. Coast Shelf Sci.* 51, 651–662. <https://doi.org/10.1006/ecss.2000.0702>.
- Wurpts, R., Torn, P., 2005. 15 Years Experience with Fluid Mud: Definition of the Nautical Bottom with Rheological Parameters. *Terra et Aqua* 99.
- Zander, F., Heimovaara, T., Gebert, J., 2020. Spatial variability of organic matter degradability in tidal Elbe sediments. *J. Soil Sediment.* 20, 2573–2587. <https://doi.org/10.1007/s11368-020-02569-4>.
- Zander, F., Shakeel, A., Kirichek, A., Chassagne, C., Gebert, J., 2022. Effects of organic matter degradation in cohesive sediment: Linking sediment rheology to spatio-temporal patterns of organic matter degradability. *J. Soil Sediment.* <https://doi.org/10.1007/s11368-022-03155-6>.